

Copyright is owned by the Author of the thesis. Permission is given for a copy to be downloaded by an individual for the purpose of research and private study only. The thesis may not be reproduced elsewhere without the permission of the Author.

PALEOSEISMOLOGY, SEISMIC HAZARD AND VOLCANO-TECTONIC INTERACTIONS IN THE TONGARIRO VOLCANIC CENTRE, NEW ZEALAND

A thesis presented in partial fulfilment of the requirements for the degree of

Doctor of Philosophy

in

Earth Science

at Massey University (Palmerston North, Manawatu)

New Zealand

By

MARTHA GABRIELA GÓMEZ VASCONCELOS

Supervisor: SHANE CRONIN

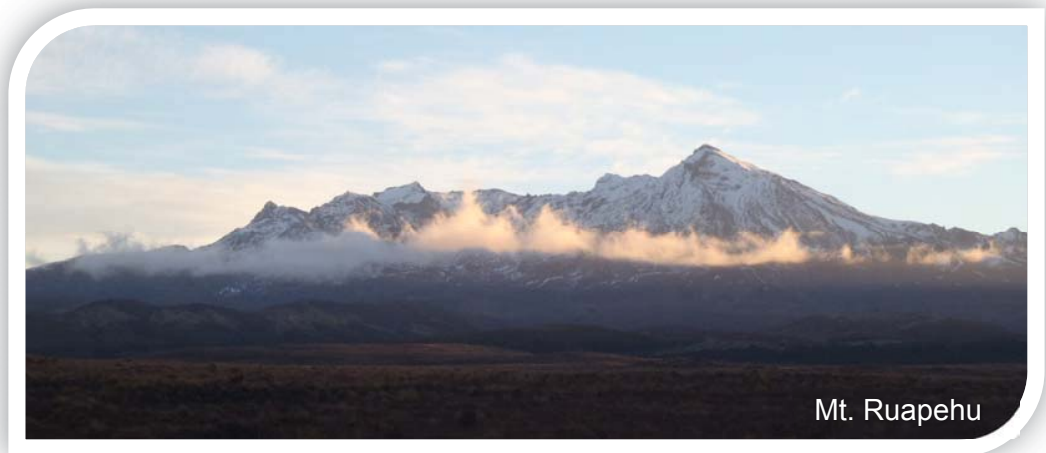
Co-supervisors: PILAR VILLAMOR (GNS Science), ALAN PALMER, JON PROCTER AND BOB STEWART



2017



To my family and Denis Avellán, who stand by me, no matter what.
I love you!



'It is not the mountain we conquer, but ourselves'. Sir Edmund Hillary

With passion, patience and persistence...

Abstract

At the southern part of the Taupo Rift, crustal extension is accommodated by a combination of normal faults and dike intrusions, and the Tongariro Volcanic Centre coexists with faults from the Ruapehu and Tongariro grabens. This close coexistence and volcanic vent alignment parallel to the regional faults has always raised the question of their possible interaction. Further, many periods of high fault slip-rate seem to coincide with explosive volcanic eruptions. For some periods these coincidences are shown to be unrelated; however, it remains important to evaluate the potential link between them. In the Tongariro Graben, the geological extension was quantified and compared to the total geodetic extension, showing that 78 to 95% of the extension was accommodated by tectonic faults and only 5 to 22% by dike intrusions. Within the latter, 4 to 5% was accommodated by volcanic eruptions and 18 to 19% by arrested dike intrusions, with an unknown percentage of hybrid extension. Short-term variations in fault slip-rates and volcanic activity for the last 100 ka in the Tongariro Volcanic Centre may have been influenced by static stress transfer between adjacent faults (within <20 km from the source) and dike intrusions (within <10 km), or by fluctuations in magma input through time. The amount of magma involved in the rifting process will condition the predominant extension mechanism and thus influence the predominant type of volcano-tectonic interaction. A record of volcanic and seismic activity for the last 250 ka was assembled, from new and published studies. This was used to analyse the spatio-temporal associations between volcanic and seismic activity in the southern Taupo Rift. Data on the faulting history, slip-rate variation and seismic hazard of the Upper Waikato Stream, Wahianoa, Waihi and Poutu faults formed the core of the analysis. These faults are capable of producing a M_w 7.2 earthquake with a single-event displacement of 2.9 m, posing an important hazard to the region. Data gathered in this study provides an update to the National Seismic Hazard Model for New Zealand.

Acknowledgments

This thesis is a very special project, accomplished with the help of very special people. I am deeply grateful to all those whose enthusiasm and support helped me get through tough times and make this dream come true.

Special thanks to Pilar Villamor, for her valuable guidance and commitment, for her shared knowledge, friendship and great assistance throughout this process.

Many thanks to my main supervisor, Shane Cronin, for his support and for giving me the opportunity to work in this project, allowing my New Zealand dream to come true.

To my supervision team, for their support throughout this experience: Pilar Villamor, Shane Cronin, Alan Palmer, Jon Procter and Bob Stewart, many thanks for the good times out in the field, for their tireless efforts to improve the manuscript, patience, lessons, discussions, support and friendship.

Thanks to the Volcanic Risk Solutions group and the Institute of Agriculture and Environment in Massey University; and to GNS science staff. To the Department of Conservation, the NZ Forest Trust, the New Zealand National Army at Waiouru and the Tongariro National Park, for allowing access to do field work. Special thanks to Kate Arentsen, Liza Haarhoff and Anja Moebis for her support and for dealing with all the administrative and exhaustive logistic issues. Also, Georg Zellmer, Gert Lube, Clel Wallace, Karoly Nemeth, Mark Bebbington, Maggi Damaschke, Rafael Torres, Szabolcs Kosik, Braden Walsh, Maricar Arpa, Eric Breard, Ermanno Brosch, Adam Neather, Manu Tost, Gabor Kereszturi, Javier Agustin and Natalia Pardo. Thanks to Dougal Townsend and Graham Leonard for providing unpublished stratigraphic data and maps; and to Salman Ashraf for providing the digital surface model.

Thanks to the financial support provided by a Massey University Doctoral Research Scholarship and by a Mexican scholarship from CONACyT. Further field support was

gratefully received via the “Learning to Live with Volcanic Risk” programme within the New Zealand Natural Hazards Research Platform.

Many thanks to my wonderful family; my parents Martha Vasconcelos and Ramón Gómez, who have taught me so much and who awoke in me the passion for volcanoes and nature, for their immense love and unconditional support; to my sisters Adriana and Mariana, my brother in law Sergio and my adorable niece Luisa, for always being so close to me and believing in me, you mean so much to me; and to all my relatives in Mexico, for their love and support.

Thanks to my friends in Palmy, my kiwi family: Javier Agustín, Diana Cabrera, Anita Mar, Patry Rubio, Majela González, Yimi Yapura, Luca Panizzi, Omar Cristobal, Angie Denes, Gabor Kereszturi, Zsuzsa Szmolinka, Szabolcs Kósik, Daniel Salazar, Cindy Chanci, Nura Majzoub, Sole Navarrete, Roberto Calvelo, Marcela Humphrey, Manu Tost, Juliana Velandia, Istvan Hajdu, Paty Alborn, Paty Ham, Mauricio Maldonado, Caro Lozada, Anai Hernandez, Pao Villacis, Kwan Maitrarat, Ceci Falla, Sam McColl, Rafa Torres, Freddy Dondin, Aniek Hilkens, Braden Walsh, Eric Breard, Laila Prae, Lovisa Ekelund, John Quintanilla, Ermanno Brosch, Vilma Rodríguez, German Molano and Alvaro Mehrle. They gave me the energy, empathy and enthusiasm I needed in good and not so good days, they made this experience more enjoyable, I will never forget them!

Thanks to my friends in México: Marthita Cortes, Vivi Ramírez, Ximena Delgado, Magda Velázquez, Susy Osorio, Diana Soria, Idana Trejo, Jennifer Marrón, Teresita Méndez, Fernando Romero, Jaime Tapia, Lucy Tapia, Judith Gasca, Pepe Moreno, Tatty Sanchez, Patty López, Mayra Díaz, Paula Perezgil, Agnes Samper, Mimí Trujillo, Adrián Jiménez, Judith Espino, Ale Huéramo, Lidia Flores, Tete Godínez, Rocy Pedraza, Monica Guizar, Adriana Cerda, Ale Gutiérrez, José Torres, Memo Cisneros, Juan Sánchez, Lupita, María López de Lara, etc.; also to my friends in Nicaragua,

USA, Europe, and other places around the world, for their support and wonderful friendship even through the distance.

Many thanks to Víctor Hugo Garduño and José Luis Macías, my first mentors, who showed me the way to science, volcanoes and faults; for their support and encouragement to discover the mysteries of geosciences.

And last, but not least, to my love, Denis Avellán, for his patience, support, encouragement and immense love he shows me every day in every way.



Table of Contents

ABSTRACT	iii
ACKNOWLEDGMENTS	iv
TABLE OF CONTENTS	vii
LIST OF FIGURES	x
LIST OF TABLES	xvii
LIST OF ABBREVIATIONS	xix
CHAPTER 1. INTRODUCTION	1
1.1 Research problem and motivation	1
1.2 Objectives	5
1.3 Thesis outline	6
CHAPTER 2. LITERATURE REVIEW AND STUDY AREA	9
2.1 Paleoseismology	9
2.2 Volcanic Rifts	10
2.2.1 Morphology of faults in volcanic rifts	10
2.3 Dike Intrusion and emplacement	13
2.3.1 Volcanic load as an influence on fault and dike patterns	16
2.3.2 Seismogenic depth as an influence on dike patterns	17
2.4 Volcano-tectonic interactions	19
2.4.1 Historical examples of volcano-tectonic interactions	22
2.5 The study area: The Tongariro Volcanic Centre	27
2.5.1 Active Tectonics of New Zealand	27
2.5.2 Regional Geology	30
2.5.2.1 The magmatic system of the TgVC	31
2.5.3 Structural Geology	36
2.5.4 Eruptive History	39
2.5.4.1 Stratigraphic summary	44
2.6 Magma-tectonic interactions in the North Island	47
CHAPTER 3. METHODOLOGY	49
3.1 Desk study methods	49
3.2 Fieldwork methods	50
3.3 Data analysis methods	53
CHAPTER 4. RESULTS: Earthquake history at the eastern boundary of south Taupo Volcanic Zone.	57
4.1 Abstract	59
4.2 Introduction	59
4.3 Geological and structural setting	60
4.4 Volcanic history and stratigraphy	62
4.5 Active faulting: the Rangipo and Wahianoa faults	64
4.6 Methods	66
4.7 Results of paleoseismic analysis	71
4.7.1 Upper Waikato Stream Fault	71
4.7.2 Wahianoa Fault	82
4.8 Discussion	84
4.8.1 Is the Upper Waikato Stream Fault part of the Rangipo Fault or part of the Wahianoa Fault?	84
4.8.2 The role of the Wahianoa, Upper Waikato Stream and Rangipo faults in	

the kinematics and evolution of the Taupo Rift	88
4.8.3 Seismic hazard from the Upper Waikato Stream and Wahianoa faults	90
4.8.4 Potential association of volcanism with periods of accelerated seismic activity	93
4.9 Conclusions	94
CHAPTER 5. RESULTS: Earthquake history and Crustal Extension in the Tongariro Graben, New Zealand: Insights into Volcano-tectonic Interactions and Active Deformation in a young Continental Rift.	97
5.1 Abstract	99
5.2 Introduction	100
5.3 Regional Geology	104
5.4 The Tongariro Graben	106
5.5 Methods	108
5.5.1 Fault Mapping and Update of GNS Active Fault Database	109
5.5.2 Fault Geometry and Displacements and Earthquake History	109
5.5.3 Slip-rates and Extension Rates	111
5.6 Results	112
5.6.1 Paleoseismology Analysis	112
5.6.1.1 Rift bounding faults: National Park and Upper Waikato Stream faults	112
5.6.1.2 The Waihi Fault Zone	114
5.6.1.3 The Poutu Fault Zone	115
5.6.2 Fault slip-rates in the Tongariro Graben	117
5.6.3 Dike intrusion rates in the Tongariro Graben	119
5.7 Discussion	120
5.7.1 Is Surface Faulting Associated with Tectonic or Dike Intrusion Processes in the Tongariro Graben?	120
5.7.2 Proportion of Extension Accommodated by Faulting vs. Dike Intrusion	126
5.8 Conclusions	129
CHAPTER 6. RESULTS: Seismic Hazard Analysis of the Tongariro Graben.	131
6.1 Abstract	132
6.2 Introduction	133
6.3 Methods	137
6.4 Results	138
6.4.1 Fault geometry	138
6.4.2 Fault slip-rates	139
6.5 Discussion	141
6.5.1 Fault segmentation	141
6.5.2 Magnitude and recurrence interval of potential earthquakes	147
6.6 Conclusions	148
CHAPTER 7. RESULTS: Spatio-temporal associations between dike intrusions and fault ruptures in the Tongariro Volcanic Centre, New Zealand.	151
7.1 Abstract	152
7.2 Introduction	152
7.3 Tectonic and geological setting	156
7.4 Previously identified volcano-tectonic interactions in the Taupo Rift	157
7.5 Methods	159
7.6 Results	161

7.6.1 Fault slip-rate changes and volcanic activity in the TgVC	161
7.6.2 Eruption volumes	163
7.6.3 Spatio-temporal associations in the TgVC	165
7.6.4 Scenarios for volcano-tectonic interactions in the TgVC	167
7.6.5 Coulomb stress transfer models	169
7.7 Discussion	175
7.7.1 Volcano-tectonic interactions by stress transfer	175
7.7.2 Controlling factors on volcano-tectonic interactions in the TgVC	181
7.7.3 Implications for natural hazards	184
7.7.4 Limitations of this study	184
7.8 Conclusions	186
 CHAPTER 8. CONCLUSIONS: Understanding mechanical coupling between volcanic unrest and large earthquakes in the Tongariro Volcanic Centre.	188
8.1 Summary	188
8.2 Tongariro and Ruapehu grabens	191
8.3 Methodologies used: advantages and disadvantages	192
8.4 Fulfilment of study objectives and additional contributions	194
8.5 Future challenges	197
 REFERENCES	199
 APPENDICES	219
Appendix A. Supplementary data	
A1. Fault Database and ArcMap shapefile	
A2. Supplementary figures	
A3. Supplementary tables	
A4. Journal publication	
A5. Extended abstract	
Appendix B. Statements of contribution	

List of Figures

- Figure 1. North Crater and Blue Lake viewed from Red Crater on the Tongariro Crossing Track. (4)
- Figure 2. Main parameters controlling dike emplacement (from Acocella and Neri, 2009). (13)
- Figure 3. Schematic illustration showing the pattern of dike emplacement and type of volcanoes when horizontal tectonic stress is compressional (a) and tensional (b). * (star), depth of brittle-ductile boundary. The shaded parts below the brittle-ductile boundary in 'a' denote magma chambers (Kurokawa et al., 1995). (14)
- Figure 4. Mead's Wall dike (2-4 m wide) at Whakapapa ski field on the northern flanks of Mt. Ruapehu, view looking north at 1678 m elevation. (15)
- Figure 5. Ngāuruhoe volcano and Tongariro Volcanic Complex viewed from Mt. Ruapehu, view approximately to the north. (23)
- Figure 6. Tectonic setting of New Zealand (from Wallace et al., 2004). Yellow dashed line shows the location of the Taupo Volcanic Zone and yellow arrows show the variation of extension rate along the rift, values in mm/yr (Wallace et al., 2004). Black arrows show Pacific/Australia relative motion in New Zealand (DeMets et al., 1994). MFS, Marlborough Fault System; NIDFB, North Island Dextral Fault Belt; TVZ, Taupo Volcanic Zone; BR, Buller regional faults; CEFZ, Cape Egmont Fault Zone. (25)
- Figure 7. Location map of the Tongariro Volcanic Centre (B) as defined by Cole (1978), and its main volcanic structures within the Taupo Volcanic Zone (TVZ) in the central North Island of New Zealand (A), as described by Gregg (1960). SC, Saddle Cone; TL, Tama Lakes; Ng, Ngāuruhoe; Pk, Pukekaikiore; P, Pukeonake; MTg, Mt. Tongariro; RC, Red Crater; TM, Te Maari; NC, North Crater; Mg, Maungakatote; Ku, Kuharua. (29)
- Figure 8. Geological map of the Tongariro Volcanic Centre in New Zealand (modified from QMap; Lee et al., 2011). (30)
- Figure 9. Late Quaternary active fault traces of the Tongariro Volcanic Centre; the northern part delimits the Tongariro Graben and the southern part the Ruapehu Graben (this work; Litchfield et al., 2013; Villamor and Berryman, 2006b). (33)
- Figure 10. General Stratigraphic sequence showing the chronology of the main lahars, tephras and lava flows in the TgVC, and some important rhyolitic stratigraphic markers. (41)
- Figure 11. The Tongariro Volcanic Centre, showing the main faults and volcanic vents, and the four main field sites focused upon for detailed fieldwork within this study. (47)
- Figure 12. Mt. Ruapehu seen from one of the main river exposures in the Upper Waikato Stream, showing a sequence of tephra units and coarse lahar deposits that record the last ~50 ka of deposition (Cronin et al., 1996b). (52)
- Figure 13. A, Tectonic setting of New Zealand. Green rectangle marks location of Figure 1B. B, Location of the Taupo Rift (active faults in red, from Langridge et al., 2016). Yellow rectangle marks location of Figure 1C. C, Location map of the Mt. Ruapehu Graben, Upper Waikato Stream (UWS), Wahianoa and Rangipo faults in the southern part of the Tongariro Volcanic Complex, in the southern Taupo Rift. Potential intersection area marked with a purple rectangle (UWS). (56)

Figure 14. Chronological stratigraphic summary of the laharic and lava formations and andesitic tephtras from the Tongariro Volcanic Centre interbedded with distal rhyolitic tephtras from the Taupo Volcanic Zone calderas. Note the general stratigraphic record for the Upper Waikato Stream and Wahianoa Fault areas at the right. *The oldest laharic formations' ages are based on the Rotoehu ash age (45.16 cal ka BP; Danišik et al., 2012). Ru, Ruapehu; Tg, Tongariro; Ng, Ngāuruhoe; Tp, Taupo; Ok, Okataina, R# corresponds to the lahar episodes as described by Cronin & Neall (1997). (59)

Figure 15. Geological map and general stratigraphy of the SE Mt. Ruapehu area (after Lee et al., 2011; Townsend et al., 2008), showing the location of the study sites (sections 1–3) and active surface fault traces (Langridge et al., 2016). See Figure 14 for detailed stratigraphic record. (61)

Figure 16. Terrestrial laser scanning survey. A, Upper Waikato Stream (UWS) 3D point cloud data. B, Oblique view of the digital outcrop model of the wall 'a' in the Upper Waikato Stream Fault built with 3DReshaper Application. C, Satellite image (using Google Earth images, 2015) showing the scanning locations and river exposures (walls) for the terrestrial laser scanning survey in the Upper Waikato Stream, section 1 (see location on Figure 15). (65)

Figure 17. Location of the main faults in the Upper Waikato Stream area. A, Hillshade map of the Upper Waikato Stream based on 2 m digital surface model showing the studied faults in sections 1 (green rectangle) and 2 (blue dots, blue rectangle). Fault exposures (dots) and fault traces (continuous lines) are differentiated from the inferred faults (discontinuous lines). Faults downthrown to the NW are marked with red lines; faults downthrown to the SE are marked with yellow–brown lines. The fault planes are plotted in stereographic (lower hemisphere) projection and superimposed rose diagrams of fault strike frequency (right-hand rule). B, Section 1 of the Upper Waikato Stream (green rectangle in A) showing the seven main fault traces (purple dots), as well as an extensional fracture and two transects t1 and t2 (white lines) used to sum and calculate the total offset for the Upper Waikato Stream Fault. (71)

Figure 18. Faults in section 1 in the Upper Waikato Stream. A, Wall 'a' main fault exposure, showing fault 1 displacing volcanic deposits older than c. 28 ka (left, field photo; right, interpretation with stratigraphic column). B, Wall 'b' showing the location of fault 2 with a 0.3 m 'fissure fill' (left, field photo; right, interpretation with stratigraphic column). C, Detailed exposure of fault 4 on wall 'b' displacing tephtras older than R11 lahars. The numbers show the elevation in m a.s.l. See Figure 14 for further information about stratigraphic units. (72)

Figure 19. Extensional fractures located on wall 'a' in the Upper Waikato Stream. A, The 12 m long fissure filled with Ōruanui Tephra (white arrow; >25.4 cal ka BP; photo taken by S. Donoghue), cutting older tephtras and lahar deposits. B, Other fissures were measured on the same wall, cutting R11 lahars. C, These fissures do not show any vertical displacement, but record extension. D, The R11 lahar deposits are abruptly truncated at the fissure margins, with no mixed material along fissure sides. The reworked Ōruanui tephtra shows cross-bedding stratified layers. E, All the fissures reflect orthogonal extension and are consistent with the NNE-trending Mt. Ruapehu Graben. Rose diagrams for the measured fissures and faults in the Tongariro Volcanic Centre (TgVC), where strike directions (right-hand rule) are plotted. (74)

Figure 20. Main outcrops of the Upper Waikato Stream Fault in section 2. A, 10/4_2: Normal fault displacing the Papakai Formation. B, 10/4_3: Exposure of fault displacing deposits including R13 and older lahars. (76)

Figure 21. Wahianoa Fault profiles and outcrops. A, Geological map [Leonard et al., 2014] showing the location of the studied field sites along the Wahianoa Fault in section 3; and the 10 topographic profiles (black double-pointed arrows) traced with their corresponding vertical offset

values in meters. The geological map overlies a hillshade created with a 2 m-resolution Digital Surface Model from the SE flank of Mt. Ruapehu. B–C, The two main outcrops of the Wahianoa Fault in section 3 showing displaced tephra (field locations shown on Figure 22A). The fault planes are plotted in stereographic (lower hemisphere) projection and superimposed rose diagrams of fault strike frequency (right-hand rule). Most of the tephra belongs to the Bullock Formation from Mt. Ruapehu (Donoghue and Neall, 2001; Pardo et al., 2012). See Figure 14 for more information about the stratigraphy and Figure 15 for location of section 3. (78)

Figure 22. Fault slip-rate variation from >45 ka to present day for the Rangipo Fault (green square) (Villamor et al., 2007), the Wahianoa Fault (based on profiles, grey circle), and the Upper Waikato Stream Fault (blue circle minimum values and orange circle maximum values). Higher slip-rate periods are coincident with the Bullock Formation, the Pahoka–Mangamate eruptions (PM), the Orange lapilli and marker unit 2 (Elephant surge) from Mt. Ruapehu, and the Ōruanui eruption from Taupo. Taupo pumice (TP) eruption is indicated at 1.72 cal ka BP. Zero (0) indicates the present day. (83)

Figure 23. Potential physical intersections and rupture models of the Upper Waikato Stream Fault with Rangipo and Wahianoa faults. A, Independent ruptures. B, Potential rupture of the Wahianoa (WF) and Upper Waikato Stream (UWS F) faults (27 km). C, Potential rupture of the Rangipo (RF), Upper Waikato Stream and Kaimanawa (Kai F) faults (43 km). (87)

Figure 24. Ngāuruhoe volcano, Pukekaikio and Mt. Ruapehu from the Mangatepopo moraine, view roughly to the south (by Anja Moebis). (92)

Figure 25. Similar geomorphic expression of volcanic rift zones in the Tongariro Graben (A) and the Asal Rift in Djibouti (B), showing parallel normal faults bounding the western and eastern flanks of the volcanic vents (modified from Stein et al., 1991). (96)

Figure 26. A, Location map of the Taupo Rift in the North Island of New Zealand (green rectangle). B, Location of the Tongariro Volcanic Centre (TgVC, yellow rectangle) at the southern part of the Taupo Volcanic Zone. Variation of extension rate along the rift, marked with black arrows, values in mm/yr (Wallace et al., 2004). Large ($M_w > 3$) and shallow (<40 km) earthquakes marked with red circles, compiled from the New Zealand catalogue of earthquakes since the 1930s (extracted from NZ GeoNet database <http://info.geonet.org.nz/display/appdata/Earthquake+Catalogue>). C, Location of the Tongariro Volcanic Complex (TVC) at the Tongariro Graben axis, the Waihi Fault (WF) and the Poutu Fault (PF) zones, Mt. Ruapehu, Ruapehu Graben and the main volcanic vents in the region. The active faults are marked in red (Langridge et al., 2016). Ng, Ngāuruhoe. (100)

Figure 27. Geological map (Leonard et al., 2014) overlain with the faults of the Tongariro Graben; the Waihi and Poutu fault zones in the graben axis area and fault traces (red lines), inferred fault traces (dotted red lines), possible scarps (black lines) and 229 vertical fault displacements (2 northern National Park Fault, 117 Waihi Fault and 110 Poutu Fault; see displacement values in Tables S3 and S4) measured from geomorphic surfaces on transverse profiles across the faults (black and green dots, values in meters). Seventeen transects (T1–T17) are marked with white lines. Field points are marked with purple dots and white numbers (referred to as Tong # in the text and figures, Table S5). (108)

Figure 28. Field outcrops from the Waihi Fault. A, Tong 70: Normal fault (F5a) displacing the Pukekaikio lava flows (190–25 ka; Hobden et al., 1996; Leonard et al., 2014), the Mt. Tongariro lava flows and the Mangatepopo moraine in Mt. Tongariro. B, Tong 78: F4b exposure displacing the Mangatawai tephra (3.52 cal ka BP; Moebis et al., 2011) and the Papakai Formation (11.1–3.7 cal ka BP; Donoghue et al., 1995; Figs. 27 and S5; Tables S5 and S7)(110)

Figure 29. Field outcrops from the Poutu Fault. A, Tong 11: three-step normal fault displacing the Pahoka and Okupata-Pourahu tephras. B, Tong 77: Multiple-step normal fault (F2b) displacing the Okupata-Pourahu tephras (11.77 ± 0.19 cal ka BP; see stratigraphy in Table S10 and locations in Figure 27, and Tables S5 and S9). (111)

Figure 30. Simplified schematic diagrams showing the variety of extension modes in continental rifts. A, Pure tectonic extension by normal faulting (unrelated to volcanism). B, Pure volcanic extension by dike intrusion and eruption (dike reaches the surface). C, Extension through both normal faulting and dike intrusion-eruption. D, Pure volcanic extension by shallow arrested dike-intrusion with associated surficial normal faults (large ground surface displacements are common). E, Hybrid extension through deep dike-intrusion and triggered normal faults (large surface displacements are related to tectonic faulting; if faulting is only related to dike-intrusion ground surface displacements are too small to be observed). F, Extension is a combination of tectonic faulting, dike intrusion-eruptions and arrested dike-intrusion. E, Extension; ET, Tectonic Extension; EV, Volcanic Extension; EAD, Arrested dike extension. (116)

Figure 31. Static displacement caused by an intruding dike projected onto cross sections. A, 1 m-wide dike intruding to the surface and causing no surface deformation; B, 1 m-wide intruding dike at 2 km depth intersecting with 30° dip faults, showing a maximum of 0.5 m of surface deformation. C, 1 m-wide intruding dike at 5 km depth intersecting with 50° dip faults, showing a maximum of 0.25 m of surface displacements. D, 1 m-wide intruding dike at 10-15 km depth intersecting with $60-70^\circ$ dip faults representing the most likely scenario for the Waihi and Poutu faults, showing no surface deformation. NPF, National Park Fault; UWSF, Upper Waikato Stream Fault. E, 20 m-wide dike representing total width of repeated dike intrusions in 20 ka; here the dike is intruding to the surface and causing no surface deformation. F, 20 m-wide intruding dike at 2 km depth intersecting with 30° dip faults, showing a maximum of 6 m of surface deformation. G, 20 m-wide intruding dike at 5 km depth intersecting with 50° dip faults, showing a maximum of 4 m of surface displacement. H, 20 m-wide intruding dike at 10-15 km depth intersecting with $60-70^\circ$ dip faults representing the most likely scenario for the Waihi and Poutu faults, showing 1.5 m of surface deformation. I and J, 1 m-wide dike intruding at 10-15 km depth showing normal stress changes ($\Delta\sigma_n$; bar, unclamping positive) projected onto cross section (A-B) showing positive stress change (red colour) on top of the intruding dike, where the Waihi and Poutu faults are. (120)

Figure 32. Shallow seismicity in New Zealand (GeoNet, <http://info.geonet.org.nz/display/quake/Earthquake>). (125)

Figure 33. A, Location map of the Taupo Rift in the North Island of New Zealand. B, Location of the Tongariro Graben and the Tongariro Volcanic Complex at the southern section of the Taupo Volcanic Zone. 229 vertical fault displacements (2 northern National Park Fault, 117 Waihi Fault and 110 Poutu Fault) measured by geomorphic surfaces on transverse profiles over the faults (values in meters). Seventeen transects marked with white lines (T1-T17). Field points marked with purple dots and white numbers (referred to as Tong # in the text and figures). UWS, Upper Waikato Stream. For more details about displacements, lithology and surface ages see Chapter 5, Tables S3 and S4. (130)

Figure 34. Measured individual fault strand displacements for different age surfaces along the strike of the Waihi and Poutu fault zones. Waihi Fault zone shows greater displacements to the north of the Tongariro Graben. (138)

Figure 35. Potential segment surface-length rupture models for the Waihi and Poutu faults, marked with purple and green lines, respectively. Ng, Ngāuruhoe; RC, Red Crater; NC, North Crater; Ph, Pihanga. (140)

Figure 36. Stormy Point look-out, Manawatu, showing sequences of river terraces from 400 to 12 ka. (145)

Figure 37. A, Location of the Taupo Volcanic Zone in the North Island of New Zealand. B, Tongariro Volcanic Centre in the southern sector of the Taupo Volcanic Zone. Location of the main regional volcanoes and faults (red lines) (Chapter 5; Langridge et al., 2016; Villamor and Berryman, 2006b). Ng, Ngāuruhoe; Tg, Mt. Tongariro; Ot, Oturere; NC, North Crater; UWS, Upper Waikato Stream. (149)

Figure 38. Summed vertical displacements across the Tongariro Graben for the last 100 ka (Waihi and Poutu faults). (156)

Figure 39. Variations in short-term fault slip-rates for various faults in the TgVC from 100 ka to the present-day (zero), showing a temporal association with regional volcanic activity and Taupo caldera eruptions (Hajdas et al., 2006; Hogg et al., 2011; Lowe et al., 2013; Vandergoes et al., 2013; Wilson et al., 2009). UWS, Upper Waikato Stream Fault; TVZ, Taupo Volcanic Zone; PM, Pahoka-Mangamate sequence at ~11 cal ka BP; BF, Bullot Formation; MF, Mangawhero Formation; Tg, Mt. Tongariro; Ot, Oturere lavas. (157)

Figure 40. Eruptive volumes of the main tephras and lava flows in the TgVC (Table S11). Mt. Ruapehu sourced deposits in blue and Tongariro Volcanic Complex in green. Ng, Ngāuruhoe (Moebis et al., 2011); PM, Pahoka-Mangamate sequence (Nairn et al., 1998); WhF, Whakapapa Formation (Conway et al., 2016); BF, Bullot Formation (Pardo et al., 2012); MF, Mangawhero Formation (Conway et al., 2016); TWLF, Te Whaiau Laharic Formation (Lecointre et al., 2002); WLF, Whangaehu Laharic Formation (Keigler et al., 2011); Tg, Mt. Tongariro (Hobden et al., 1996); Ot, Oturere (Hobden et al., 1996); WF, Wahianoa Formation (Gamble et al., 2003); Pk, Pukekaikiore (Hobden et al., 1996); THF, Te Herenga Formation (Conway et al., 2016); TL, Tama Lakes (Hobden et al., 1996). (158)

Figure 41. Spatio-temporal associations for the Tongariro Volcanic Centre from known paleo-earthquakes (fault slip-rates and events) and volcanic eruptions for six different periods, showing their variation in activity for the last 250 ka. The triangles are the volcanic vents and the lines are the faults. R, Ruapehu; TL, Tama Lakes; Ng, Ngāuruhoe; Tg, Mt. Tongariro; Ot, Oturere; NC, North Crater; TM, Te Maari; Pk, Pukekaikiore; Pn, Pukeonake; P, Pihanga; KT, Kakaramea-Tihia; Hg, Hauhungatahi; OC, Ohakune Craters; HC, Half Cone; NP F, National Park Fault; UWS F, Upper Waikato Stream Fault. At time 4 there was a major caldera forming eruption at Taupo caldera: the Ōruanui ignimbrite at 25.4 cal ka BP (Vandergoes et al., 2013).

(160)

Figure 42. Scenarios for volcano-tectonic, volcano-volcano and fault-fault interactions in the Tongariro Volcanic Centre (marked in red) for six different periods in the last 250 ka based on regional spatio-temporal associations from fault slip-rates and volcanic eruption volume changes (Fig. 41). (162)

Figure 43. Stress change models with different source faults. Red areas are positive, where the stress changes are likely to encourage a fault rupture or a dike intrusion on the receiver fault or dike. Green lines represent faults on surface and red lines represent faults at depth. A, Negative normal stress change on Ngāuruhoe and other dikes in the Tongariro Volcanic Complex, and positive normal stress change on Mt. Ruapehu after a Waihi Fault rupture. B, Negative normal stress change on the Tongariro Volcanic Complex dikes, and positive normal stress change on Mt. Ruapehu after a Poutu Fault rupture. C and D, Positive Coulomb stress change on Rangipo, Upper Waikato Stream (UWS) and Ohakune faults after a Wahianoa Fault rupture. E, Negative normal stress change on Mt. Ruapehu after a Wahianoa Fault rupture. (165)

Figure 44. Stress change models from different source faults. A and B, Positive Coulomb stress change on Wahianoa and Upper Waikato Stream (UWS) faults after a Rangipo Fault rupture. C, Negative normal stress change on Mt. Ruapehu after a Rangipo Fault rupture. D, Positive Coulomb stress change on Wahianoa Fault after an Ohakune Fault rupture. E, Positive Coulomb stress change on the Wahianoa Fault after an Upper Waikato Stream Fault rupture. F, Positive Coulomb stress change on the Rangipo Fault after an UWS Fault rupture. (167)

Figure 45. A, Negative Coulomb stress change on Wahianoa and southern Waihi faults, and positive stress change on southern Poutu Fault and Tama Lakes dikes after a NNE-SSW Ruapehu dike intrusion. B, Positive stress change on southern Waihi and Poutu faults, southern Wahianoa Fault and Tama Lakes dikes, and negative stress change on northern Wahianoa Fault after a N-S Mt. Ruapehu dike intrusion. C, Positive stress change on Poutu Fault and Tama Lakes dikes, and negative stress change on Waihi and Wahianoa faults after an E-W Mt. Ruapehu dike intrusion. D, Positive Coulomb stress change on Waihi and Poutu faults after a NNE-SSW Tongariro Volcanic Complex dike intrusion. E, Positive normal stress change on Ngāuruhoe, Te Maari, Tama Lakes and Ruapehu dikes after a Tongariro Volcanic Complex dike intrusion. (168)

Figure 46. Possible scenarios for dike-fault, dike-dike and fault-fault interactions by stress transfer in the Tongariro Volcanic Centre for the last 250 ka after evaluating the Coulomb and normal stress change models (Figs. 43-45), where the red colour denotes a positive stress change and the blue colour a negative stress change. (169)

Figure 47. Combination of tectonic and magmatic extension in the Tongariro Graben. Fault slip-rate variation could be explained by different tectonic and magmatic input to the total extension. Input can fluctuate through time but total extension remains constant. Magmatic input could vary from 22 to 5% and tectonic input from 95 to 78% of the total extension (Chapter 5). (177)

Figure 48. Mt. Ruapehu volcano from Waihohonu moraine (June 2014 by Agnes Samper). (210)

Supplementary figures

Figure S1. Main river exposures (walls) in the Upper Waikato Stream at section 1 showing the studied faults (red lines). Location of the walls can be seen on Figure 16.

Figure S2. Faults in section 1 in the Upper Waikato Stream. A, Image from Cyclone software showing fault 3 on 'wall b' and its general stratigraphy. B, Fault 3 on 'wall c' showing a three-step fault scarp. C, D & E, Southern corner of 'wall b' showing exposure of fault 4 and general stratigraphy. F, Exposure of fault 5 on 'wall c' showing multiple-step fault on R11 lahars. G, Cyclone measurement of fault 5 on 'wall b' on R11 lahars. H, Exposure of the termination of fault 5 on the Hokey Pokey eruptive period on 'wall c'. I, 'Wall d' with a multiple-step fault (6) cutting through R11 lahars. J, Fault 7 exposure cutting through elephant surge up to R11 lahars with a multiple-event step-fault. See Figure 14 for further information about stratigraphic units.

Figure S3. A, Fault 10/4_1:030/65SE to 055/85NW normal fault, vertical offset ~1 m; and a secondary fault 010/76NW with 0.77 ± 0.16 m of net-slip. The stratigraphic position and the fault termination of this fault are uncertain. B, 10/4_2: normal step-fault cutting through the Papakai Formation. C, 10/4_4b: fault exposure cutting through R13 lahars and older deposits. D, 10/4_4a: Fault exposure 10 m above the river level. E, 10/4_4b: Fault exposure 2 m above the river level cutting through the Okataina sourced Rotoehu Ash (64 ka), R13 lahars, marker unit 3 and R14 lahars. F, 10/4_5: normal fault cutting R15 lahars and older deposits. G: 10/4_6: fault exposure of a normal fault cutting R13 lahars and older deposits. H, 11/4_4 and 11/4_5: faults and fractures that cut through greywackes and younger tephra, cropping out by the river level.

Figure S4. A, Wahianoa Fault outcrop 'Tong 23' in the Karioi Forest, section 3, showing antithetic faults (field location shown on Figure 21A). The fault planes are plotted in stereographic (lower hemisphere) projection and superimposed rose diagrams of fault strike frequency (right-hand rule). See Figure 14 for more information about the stratigraphy. B, Wahianoa Fault cutting across and andesite lava flow of the Mangawhero Formation.

Figure S5. Waihi Fault main field outcrops. A-D, Field outcrop 'Tong 78' showing displaced tephra mainly from the Ngāuruhoe Formation (Moebis et al., 2011) cut by fault 5. E-F, Field point outcrop 'Tong 70' showing displaced tephra mainly from the Bullot Formation from Mt. Ruapehu (Donoghue & Neall, 2001; Pardo et al., 2012) cut by fault 6.

Figure S6. Poutu Fault main field outcrops. A, Field site 'Tong 09' displaced by Poutu Fault strand F7b showing 4 m of deformation since 11 ka. B-C, Field site 'Tong 11' and 'Tong 10' showing ~11 ka displaced tephra on NE flanks of Mt. Ruapehu. D, Field outcrop 'Tong 50' on F4a Poutu Fault strand.

Figure S7. Poutu Fault main field outcrops. A-B, Field outcrops 'Tong 72' and 'Tong 73' on F1a Poutu Fault strand. C-D, 'Tong 76' and 'Tong 77' field sites showing displaced tephra between ~14 and 11 ka.

List of Tables

- Table 1. Main morphological structures that evidence a prehistoric earthquake McCalpin, 2009. (8)
- Table 2. Net-slip, single-event displacements, progressive displacements and timing of rupture of the Upper Waikato Stream Fault, at section 1. (68)
- Table 3. Net-slip, single-event displacement and timing of fault rupture of the Upper Waikato Stream Fault, at section 2. (76)
- Table 4. Net-slip, single-event displacements, progressive displacements and timing of rupture of the Wahianoa Fault, at section 3. (78)
- Table 5. Comparison of fault rupture number and timing of the Upper Waikato Stream, Wahianoa and Rangipo faults. (81)
- Table 6. Moment magnitude and single-event displacement for different fault lengths. (87)
- Table 7. Vertical displacements and slip-rates for the Tongariro Graben, from Waihi and Poutu faults transects and rift-bounding faults. (113)
- Table 8. Surface and seismogenic depth extension rates at 20 and 60 ka for the Tongariro Graben. (121)
- Table 9. Vertical displacements and slip-rates summary for the Tongariro Graben, from Waihi and Poutu faults transects and rift-bounding faults. (134)
- Table 10. Moment magnitude and single-event displacement for different fault lengths. (142)

Supplementary tables

Table S1. Net-slip, single-event displacements, progressive displacements and timing of rupture of the Upper Waikato Stream Fault, sections 1 & 2.

Table S2. Net-slip, single-event displacements, progressive displacements and timing of rupture of the Wahianoa Fault, sections 2 & 3, and comparison of fault ruptures of the Upper Waikato Stream, Wahianoa and Rangipo faults.

Table S3. Waihi Fault displacements.

Table S4. Poutu Fault displacements.

Table S5. Field locations.

Table S6. Waihi Fault, geomorphic surface offsets and progressive displacements.

Table S7. Waihi Fault, outcrop offsets and progressive displacements.

Table S8. Poutu Fault, geomorphic surface offsets and progressive displacements.

Table S9. Poutu Fault, outcrop offsets and progressive displacements.

Table S10. Main stratigraphic units.

Table S11. Magma volumes of the Tongariro Volcanic Centre.

Table S12. Co-seismic slip for the southern Taupo Rift faults.

List of abbreviations

BP	Before Present
cal	calibrated
CFC	Coulomb failure criterion
DSM	Digital Surface Model
GIS	Geographic Information System
GNS	Institute of Geological and Nuclear Sciences
GPa	Gigapascal
GPS	Global Positioning System
ka	Thousand years
Ma	Million years
m a.s.l.	Metres above the sea level
Mt.	Mount
M _w	Moment magnitude
PM	Pahoka-Mangamate
RTK	Real Time Kinematic
TgVC	Tongariro Volcanic Centre
TVC	Tongariro Volcanic Complex
TLS	Terrestrial Laser Scanning
TVZ	Taupo Volcanic Zone
UWS	Upper Waikato Stream
VEI	Volcanic Explosivity Index